In-situ immobilization of $Fe/Fe_3C/Fe_2O_3$ hollow hetero-nanoparticles onto nitrogen-doped carbon nanotubes towards high-efficiency electrocatalytic oxygen reduction

Binbin Zhang,[a] Tongfei Li,[a] Longzhen Huang,[a] Yiping Ren,[a] Dongmei Sun,[a] Huan Pang,[b] Jun Yang,[c, d] Lin Xu,*[a] and Yawen Tang*[a]

a Jiangsu Key Laboratory of New Power Batteries, School of Chemistry and Materials Science

Nanjing Normal University

Nanjing 210023, China

E-mail: xulin001@njnu.edu.cn, njuxulin@gmail.com (L. Xu); tangyawen@njnu.edu.cn (Y. Tang)

b School of Chemistry and Chemical Engineering

Yangzhou University

Yangzhou 225009, China

c Nanjing IPE Institute of Green Manufacturing Industry

Nanjing 211100, China

d State Key Laboratory of Multiphase Complex Systems

Institute of Process Engineering, Chinese Academy of Sciences

Beijing 100190, China

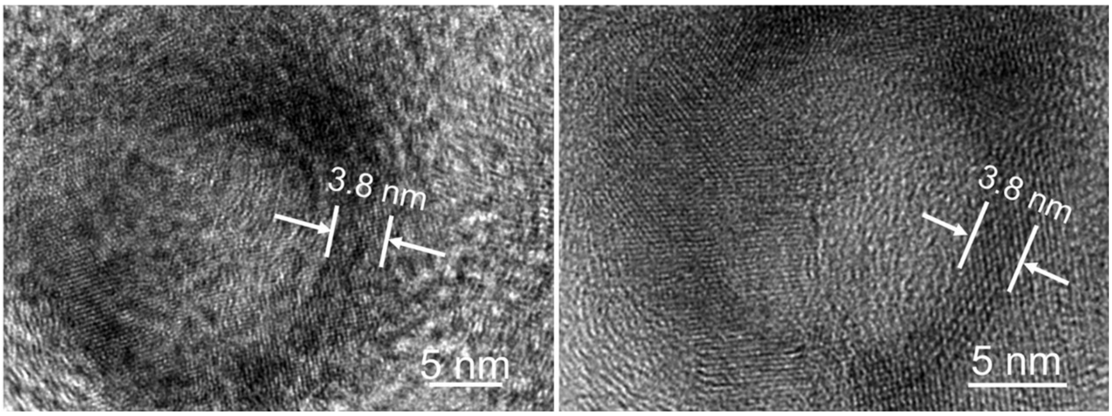

Figure S1. TEM images of $Fe/Fe_3C/Fe_2O_3$ hollow nanoparticles.

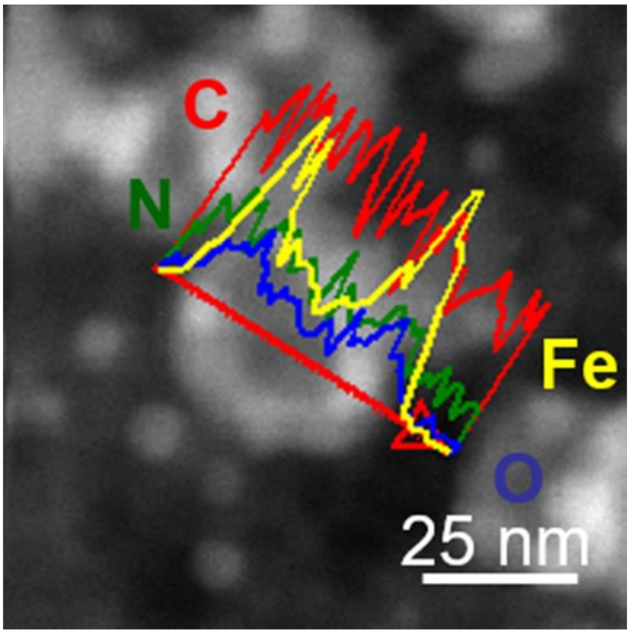

Figure S2. HAADF-STEM image and EDX line scanning profiles of $Fe/Fe_3C/Fe_2O_3$ hollow nanoparticles.

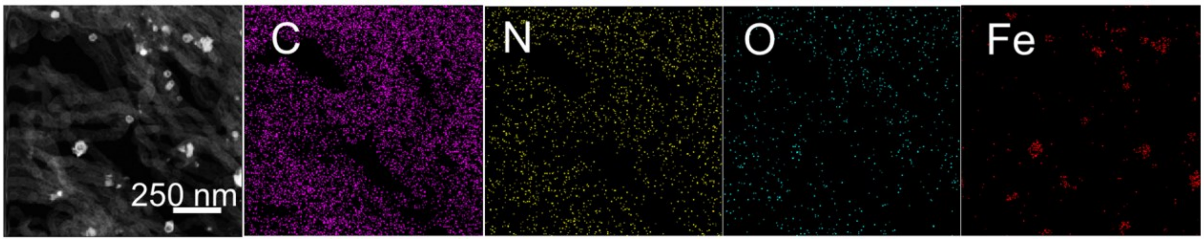

Figure S3. HAADF-STEM image and elemental mapping images of the formed $Fe/Fe_3C/Fe_2O_3$@N-CNTs.

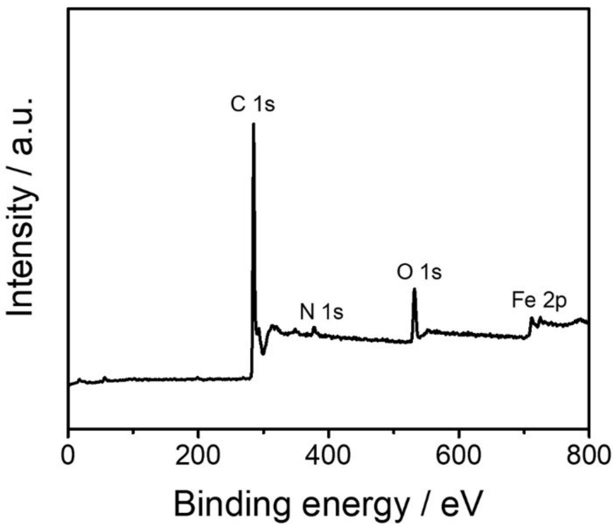

Figure S4. XPS survey spectrum of $Fe/Fe_3C/Fe_2O_3$@N-CNTs.

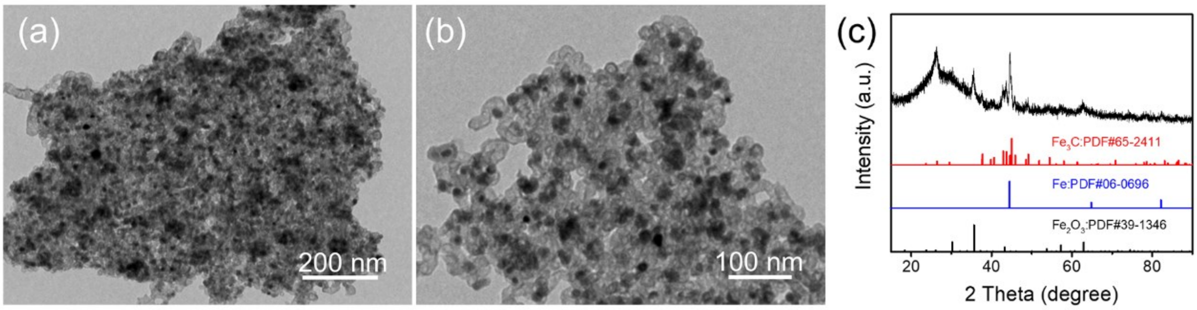

Figure S5. Morphological and structural characterization of $Fe/Fe_3C/Fe_2O_3$@N-CNTs-800. (a)-(b) TEM images, and (c) XRD pattern.

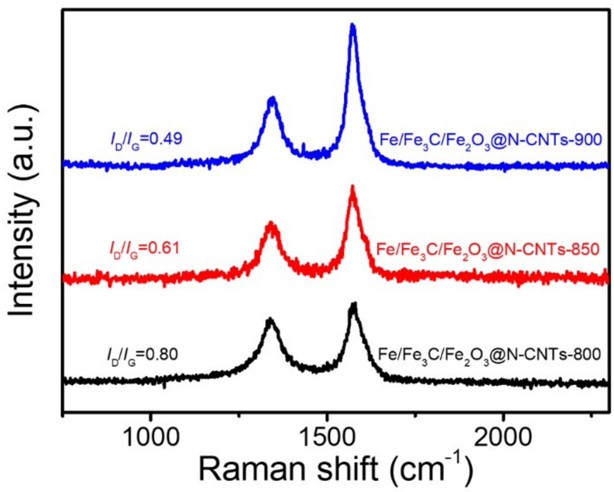

Figure S6. Raman spectra of the $Fe/Fe_3C/Fe_2O_3$@N-CNT family samples obtained at different pyrolysis temperatures.

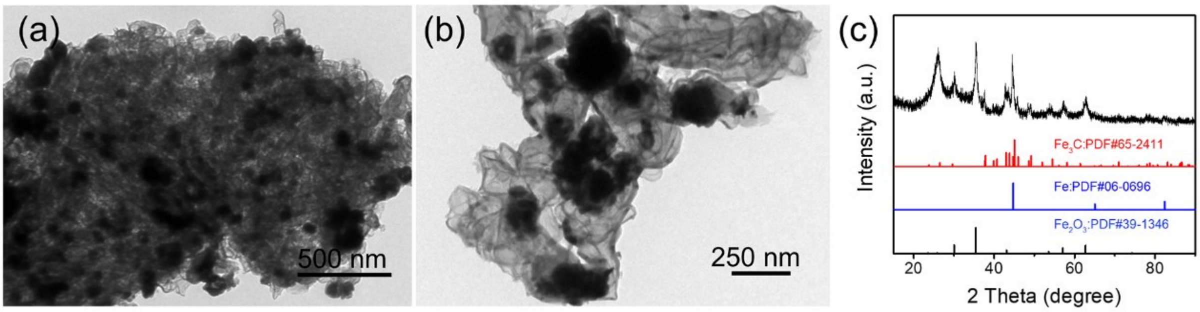

Figure S7. Morphological and structural characterization of $Fe/Fe_3C/Fe_2O_3$@N-CNTs-900. (a)-(b) TEM images, and (c) XRD pattern.

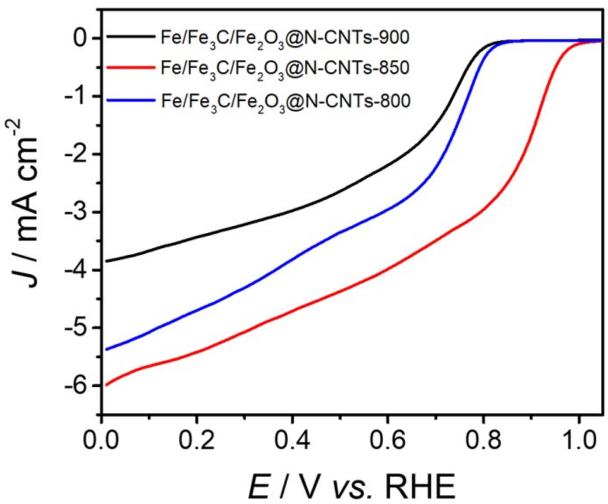

Figure S8. LSV curves of the $Fe/Fe_3C/Fe_2O_3$@N-CNT family samples obtained at different pyrolysis temperatures.

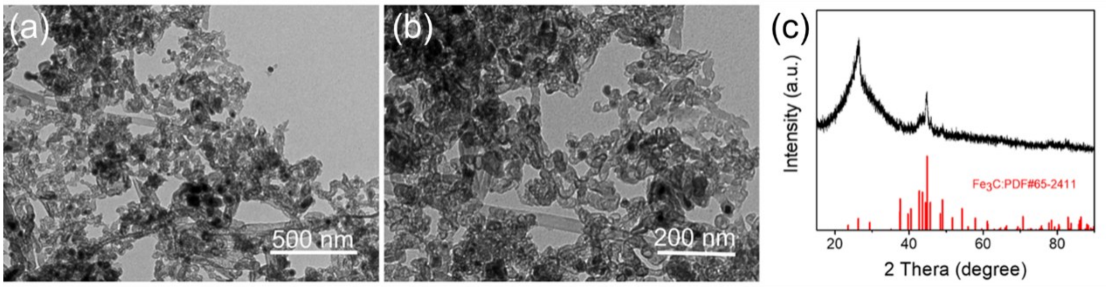

Figure S9. Morphological and structural characterization of the Fe_3C@N-CNTs. (a)-(b) TEM images, and (c) XRD pattern.

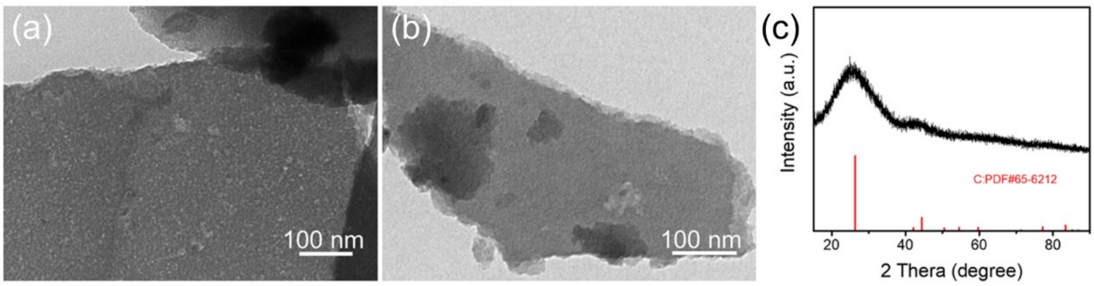

Figure S10. Morphological and structural characterization of the N-CNSs. (a)-(b) TEM images, and (c) XRD pattern.

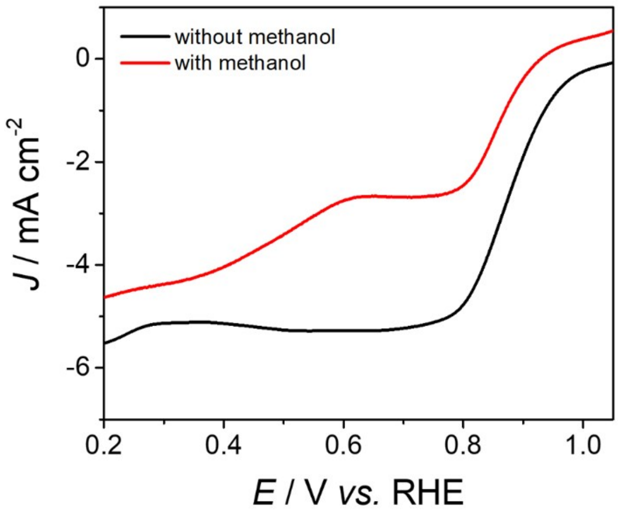

Figure S11. LSV curves of commercial Pt/C catalyst in an O_2-saturated 0.1 M KOH with and without methanol, respectively.

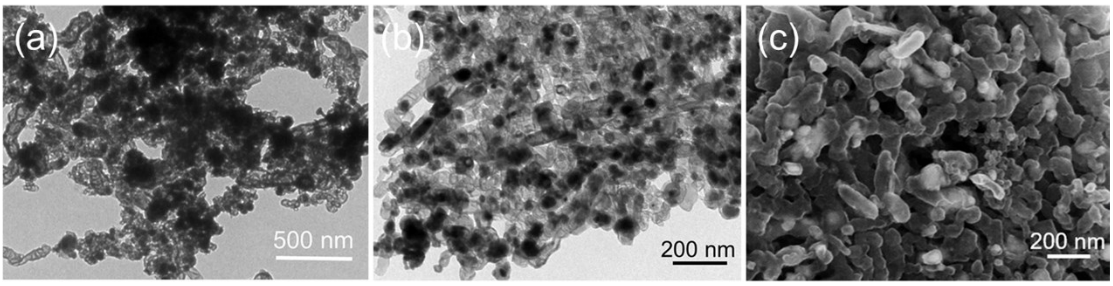

Figure S12. Morphological characterization of $Fe/Fe_3C/Fe_2O_3$@N-CNTs after the stability test. (a)-(b) TEM images, and (c) SEM image.

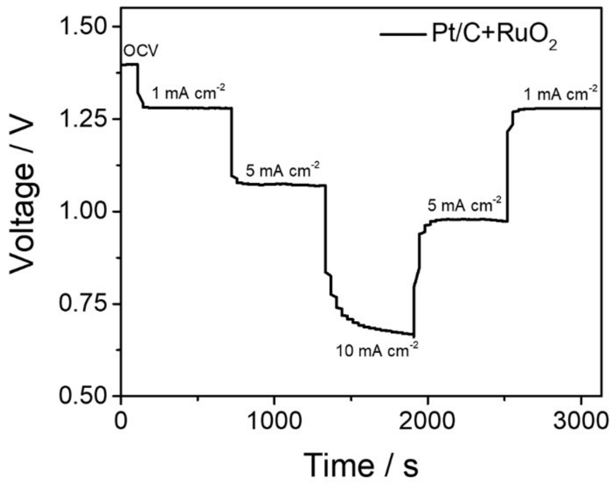

Figure S13. The rate performance of the Pt/C+RuO_2-equipped ZAB.

Table S1. Comparison of the ORR performance of the synthesized $Fe/Fe_3C/Fe_2O_3$@N-CNTs with previously reported Fe-based ORR catalysts in alkaline medium.

Electrocatalysts	E_{onset} (V *vs*. RHE)	$E_{1/2}$ (V *vs*. RHE)	Ref.
$Fe/Fe_3C/Fe_2O_3$@N-CNTs	0.985	0.890	This work
Fe@NMC-1	1.01	0.88	*ACS Appl. Mater. Interfaces,* 2019, 11, 25976
FePC-NH_2 /HCB800	0.98	0.84	*J. Energy Chem.,* 2019, 28, 73
Fe@N–C NT/NSs	1.0	0.82	*Nanoscale*, 2020, 12, 13987
Fe@C–NG/NCNTs	0.93	0.84	*J. Mater. Chem. A*, 2018, 6, 516
Fe/Fe_3C@N–C–NaCl	0.970	0.869	*J. Mater. Chem. A*, 2016, 4, 7781
FeCNR-750	0.96	0.83	*Inorg. Chem. Front.,* 2020, 7, 889
Fe_7C_3@FeNC	0.96	0.83	*ACS Sustainable Chem. Eng.,* 2019, 7, 13576
FeNPC	1.03	0.88	*J. Mater. Chem. A*, 2019, 7, 14732
Fe−N−C/MXene	0.92	0.84	*ACS Nano*, 2020, 14, 2436
Fe-CZIF-800-10	0.982	0.830	*Nanoscale,* 2018, 10, 9252
Fe-N-OCNT	0.96	0.86	*New J. Chem.*, 2020, 44, 10729
Fe/Fe_3C@N-C-1	0.936	0.804	*J. Colloid Interface Sci.*, 2018, 524, 93
FePc@N,P-DC	0.979	0.903	*Appl. Catal. B: Environ.,* 2020, 260, 118198
Fe/Fe_3C@Fe-N_x-C	1.0	0.9	*J. Energy Chem.*, 2021, 56, 72
Fe_3N@NC	0.995	0.849	*Carbon,* 2019, 153, 364

Table S2. Comparison of power density of $Fe/Fe_3C/Fe_2O_3$@N-CNTs with other previously reported Fe-based catalysts.

Catalysts	Power Density ($mW\ cm^{-2}$)	Electrolyte	Ref.
$Fe/Fe_3C/Fe_2O_3$@N-CNTs	126.7	6.0 M KOH + 0.2 M $ZnCl_2$	This work
Pt/C+RuO_2	102.6	6.0 M KOH + 0.2 M $ZnCl_2$	Commercial catalysts
Ni-Fe-MoN NTs	118	6 M KOH	*Adv. Energy Mater.,* 2018, 8, 1802327
Fe-Co_4N@N-C	105	6.0 M KOH + 0.2 M $Zn(Ac)_2$	*Appl. Catal. B: Environ.,* 2019, 256, 117893
u-Fe_7C_3@NC	105.3	7.0 M KOH + 0.2 M $ZnCl_2$	*Chem. Commun.,* 2019, 55, 5651
Fe/Co-N/S-Cs	102.63	6.0 M KOH + 0.2 M $Zn(Ac)_2$	*Appl. Catal. B: Environ.,* 2019, 241, 95
$Fe_{0.5}Ni_{0.5}$@N-GR	85	6.0 M KOH + 0.2 M $Zn(Ac)_2$	*Adv. Funct. Mater.*, 2018, 28, 1706928
Fe–N–C	100	6 M KOH	*Carbon*, 2019, 150, 475
Fe_2P/NPC	111.6	6.0 M KOH + 0.2 M $Zn(Ac)_2$	*Carbon,* 2020, 158, 885
FeO_x@N-PHCS	93.6	6.0 M KOH + 0.2 M $Zn(Ac)_2$	*J. Energy Chem.*, 2020, 49, 14
Co_2FeO_4/NCNTs	90.68	6.0 M KOH + 0.2 M $Zn(Ac)_2$	*Angew. Chem. Int. Ed.*, 2019, 58, 13291
AlFeCoNiCr	125	6.0 M KOH + 0.2 M $Zn(Ac)_2$	*Appl. Catal. B: Environ.,* 2020, 268, 118431
FC-C@NC	118.2	6.0 M KOH + 0.2 M $Zn(Ac)_2$	*Carbon Energy,* 2020, 2, 283
A-FeNC	102.2	6.0 M KOH + 0.2 M $Zn(Ac)_2$	*Phys. Chem. Chem. Phys.,* 2020, 22, 7218
Fe_2Ni@NC	126	6.0 M KOH + 0.2 M $Zn(Ac)_2$	*Adv. Energy Mater.,* 2019, 8, 1903003a